JBC ARTICLE

⌘ Author's Choice

Inhibition of the SUV4-20 H1 histone methyltransferase increases frataxin expression in Friedreich's ataxia patient cells

Received for publication, August 28, 2020 Published, Papers in Press, October 7, 2020, DOI 10.1074/jbc.RA120.015533

Gabriela Vilema-Enríquez[1], Robert Quinlan[2,3], Peter Kilfeather[1], Roberta Mazzone[2,3], Saba Saqlain[1], Irene del Molino del Barrio[1], Annalidia Donato[1], Gabriele Corda[1], Fengling Li[4], Masoud Vedadi[4,5], Andrea H. Németh[6,7], Paul E. Brennan[2,3], and Richard Wade-Martins[1,*]

From the [1]Department of Physiology, Anatomy and Genetics, the [2]Structural Genomics Consortium, the [3]Alzheimer's Research UK Oxford Drug Discovery Institute, Target Discovery Institute, Nuffield Department of Medicine, and the [6]Nuffield Department of Clinical Neurosciences, University of Oxford, Oxford, United Kingdom, the [4]Structural Genomics Consortium and the [5]Department of Pharmacology and Toxicology, University of Toronto, Toronto, Ontario, Canada, and the [7]Oxford Centre for Genomic Medicine, Oxford University Hospitals National Health Service Trust, Oxford, United Kingdom

Edited by John M. Denu

The molecular mechanisms of reduced frataxin (*FXN*) expression in Friedreich's ataxia (FRDA) are linked to epigenetic modification of the *FXN* locus caused by the disease-associated GAA expansion. Here, we identify that SUV4-20 histone methyltransferases, specifically SUV4-20 H1, play an important role in the regulation of FXN expression and represent a novel therapeutic target. Using a human *FXN*–GAA–Luciferase repeat expansion genomic DNA reporter model of FRDA, we screened the Structural Genomics Consortium epigenetic probe collection. We found that pharmacological inhibition of the SUV4-20 methyltransferases by the tool compound A-196 increased the expression of FXN by ~1.5-fold in the reporter cell line. In several FRDA cell lines and patient-derived primary peripheral blood mononuclear cells, A-196 increased FXN expression by up to 2-fold, an effect not seen in WT cells. SUV4-20 inhibition was accompanied by a reduction in H4K20me2 and H4K20me3 and an increase in H4K20me1, but only modest (1.4–7.8%) perturbation in genome-wide expression was observed. Finally, based on the structural activity relationship and crystal structure of A-196, novel small molecule A-196 analogs were synthesized and shown to give a 20-fold increase in potency for increasing *FXN* expression. Overall, our results suggest that histone methylation is important in the regulation of *FXN* expression and highlight SUV4-20 H1 as a potential novel therapeutic target for FRDA.

Friedreich's ataxia (FRDA) is the most common autosomal recessive ataxia with an estimated prevalence of 1 in 50,000 in the Caucasian population (1, 2). The disorder is caused by an unstable GAA trinucleotide repeat expansion in the first intron of the frataxin (*FXN*) gene locus (1) on chromosome 9 (3). *FXN* encodes frataxin, a protein that plays a role in mitochondrial iron–sulfur cluster biogenesis and is highly conserved across most organisms (4). The aberrant GAA expansion leads to partial transcriptional silencing of *FXN*, which results in the expression of structurally and functionally normal frataxin but at dramatically lower levels compared with the WT locus (5). In the normal *FXN* gene there can be up to 40 GAA repeats, whereas disease-associated alleles contain more than 40 GAA repeats, most commonly ~600–900. Larger GAA expansions, particularly that of the smaller allele, correlate with earlier age at onset and severity of the disease (6).

The precise mechanism by which the GAA expansion causes a partial silencing of *FXN* is still unclear. However, a wealth of studies have documented that expanded GAA·TTC repeats adopt unusual DNA structures, which are responsible for the reduced levels of frataxin. These unusual structures might produce either sticky DNA (formed by the association of two purine–purine–pyrimidine triplexes (7–11)) or persistent DNA–RNA hybrids (12) or induce the formation of repressive heterochromatin (13, 14). Furthermore, gene silencing has been recently linked to its association with the nuclear transcriptional repressive environment, the nuclear lamina (15).

In recent years, epigenetic changes such as DNA methylation or histone modifications have been implicated in a variety of diseases including FRDA (16). The GAA triplet repeat expansion was shown to silence the *FXN* locus similar to position effect variegation (13) and to be enriched in histone modifications associated with heterochromatin (H3K9me2/3, H3K27me3, H4K20me3) and conversely to have reduced acetylated histones H3 and H4, which are marks of active chromatin (16, 17). Among the histone marks associated with silent chromatin, H4K20me3 is highly enriched at telomeres and pericentric heterochromatin, as well as imprinted regions and repetitive elements, suggesting that this histone modification is involved in transcriptional silencing (18). In FRDA, the *FXN* gene carrying a GAA expansion has been shown to have increased H4K20me3 in the flanking regions of the GAA repeats (19), suggesting that the transcriptionally repressive H4K20me3 may be involved in the silencing of *FXN*. The family of histone methyltransferases SUV4-20, comprising two lysine methyltransferase enzymes SUV4-20 H1 and SUV4-20 H2, are responsible for the generation of H4K20me2 and H4K20me3 (20).

This article contains supporting information.

* For correspondence: Richard Wade-Martins, richard.wade-martins@dpag.ox.ac.uk.

Here, we report that the inhibition of the SUV4-20 histone methyltransferases, specifically SUV4-20 H1, increases FXN protein expression in a human *FXN*–GAA–Luciferase repeat expansion genomic DNA locus reporter model and in primary FRDA patient–derived cells. This novel finding highlights the importance of the methylation of H4K20 in the silencing of *FXN* and identifies the SUV4-20 H1 methyltransferase as a novel target for therapeutic intervention.

Results

Screening the structural genomics consortium epigenetic probe collection identifies histone methyltransferases as important regulators of FXN expression

High levels of specific heterochromatin marks have been previously reported at the first intron of the pathologically silenced *FXN* gene (for a review of the epigenetic changes associated with *FXN*, see Ref. 17). The epigenetic probe collection from the Structural Genomics Consortium (SGC) comprises a well-characterized set of drug-like small molecules that inhibit specific chromatin regulatory proteins and domains including bromodomains, demethylases, and methyltransferases (21, 22). To identify novel epigenetic targets involved in the regulation of *FXN* expression, we screened the SGC epigenetic chemical probe set using our *FXN*–GAA–Luc reporter cell line (15, 23) in a 96-well format in duplicate (Table S1) and assayed frataxin–luciferase (FXN–Luc) protein expression by luciferase assay (Fig. 1*A*). The screen identified five candidate compounds able to increase the expression of FXN–Luc protein above the levels of the DMSO vehicle control (Fig. 1*B*) in the absence of any toxicity assayed by the adenylate kinase assay (Fig. S1). The positive hit compounds are inhibitors of several histone methyltransferases, being SUV4-20 H1/H2 (compound 3; A-196), G9a/GLP (compound 4; A-366), EZH1/EZH2 (compound 11; GSK343), type I protein arginine methyltransferases (compound 23; MS023), and DOT1L (compound 33; SGC0946). We tested all five hit compounds in the cell line carrying an unexpanded *FXN*–Luc construct and found the molecules to increase the expression of *FXN*–Luc by approximately 2-fold (Fig. S2).

We next performed a concentration-response assay for the five hits identified in the primary screen to study the expression of *FXN*–GAA–Luc protein with increasing concentration of each chemical probe. We incubated the *FXN*–GAA–Luc cell line in a 96-well format in triplicate with increasing concentrations of the probes from 0.1 to 10 μM for 6 days. The concentration-response curves confirmed A-196, GSK343, and SGC0946 as positive hits (Fig. 1*C*), whereas A-366 and MS023 did not confirm by concentration response (Fig. S3). Four of the chemical probes exhibited no toxicity, whereas GSK343 was toxic to cells at concentrations above 5 μM (Fig. S1), and so *FXN*–GAA–Luc protein expression was only assessed from 0.1 to 5 μM of GSK343. EC_{50} values were estimated as 5.2 μM (A-196), 596 μM (GSK343), and 6.8 μM (SGC0946).

Overall, the screening of the SGC epigenetic probe collection demonstrated that inhibition of several methyltransferases acting on histones H3 and H4 may play an important role in the regulation of *FXN* expression. Furthermore, this work suggests histone methyltransferases as a novel set of potential therapeutic targets not previously studied for FRDA.

Genetic modification of the SUV4-20 family of methyltransferases reveals histone H4 lysine 20 (H4K20) methylation as a key epigenetic mark for FXN gene silencing

The screen of the SGC epigenetic probe collection highlighted the role of histone lysine methylation in *FXN* silencing. Previous reports have described the accumulation of methylation marks on lysine residues on histones H3 and H4 at the *FXN* gene (13, 19, 24–31). To validate the most promising targets, we performed siRNA-mediated knockdown of *SUV4-20H1/H2*, *EZH1/EZH2*, and *DOT1L* in the *FXN*–GAA–Luc cell line. *FXN*–GAA–Luc HEK293 cells were treated with 25 nM of siRNA for 6 days. siRNA-mediated knockdown of *SUV4-20 H1*, but not *SUV4-20 H2*, significantly increased FXN–Luc protein expression (Fig. 2, *A–D*), providing genetic validation of SUV4-20 H1 as the target of interest. However, siRNA-mediated knockdown of *DOT1L*, *EZH1*, or *EZH2* did not result in a significant increase of FXN–Luc protein expression (Figs. S4 and S5).

We then performed siRNA-mediated knockdown of *SUV4-20 H1* in the FRDA patient–derived primary fibroblast line GM04078 to confirm that the up-regulation of *FXN* following knockdown of SUV4-20 H1 is not limited to the *FXN*–GAA–Luc reporter cell line. The siRNA-mediated knockdown of *SUV4-20 H1* in primary fibroblasts increased *FXN* mRNA expression by ~1.25-fold (Fig. 2, *E* and *F*). Taken together, these results demonstrate that direct down-regulation of SUV4-20 H1 significantly increases *FXN* expression, validating this histone lysine methyltransferase as a therapeutic target for FRDA.

A-196 increases frataxin expression in FRDA patient–derived primary cells

To extend the finding that A-196 is able to increase *FXN* expression to FRDA patient cells, we treated several patient-derived cells with 5 or 10 μM A-196 for 6 days. We first treated the primary fibroblast line GM04078 and assessed mature frataxin protein expression by Western blotting (Fig. 3, *A* and *B*). Treatment with A-196 significantly increased mature FXN expression at both concentrations in this primary fibroblast line.

We next treated the FRDA patient–derived lymphoblastoid cell lines GM16220 and GM15850 with 5 or 10 μM A-196 for 6 days and measured total frataxin levels by AlphaLISA. As previously shown in fibroblasts, A-196 was able to increase significantly FXN protein expression in both lymphoblastoid cell lines (Fig. 3, *C* and *D*). We also showed that the structural inactive analog of A-196, SGC2043, did not increase frataxin protein expression, further confirming the selective and specific mechanism of action of A-196.

We next tested A-196 in primary peripheral blood mononuclear cells (PBMCs) isolated from four FRDA patients. PBMCs treated with 5 or 10 μM A-196 for 6 days increased *FXN* mRNA expression by ~2-fold assessed by qRT-PCR (Fig. 3*E*).

Finally, we treated two control-derived primary fibroblast lines, one control lymphoblastoid cell line, and PBMCs derived from three control individuals with 5 or 10 μM A-196 and assessed frataxin mRNA expression (Fig. S6). We found that A-196 does not

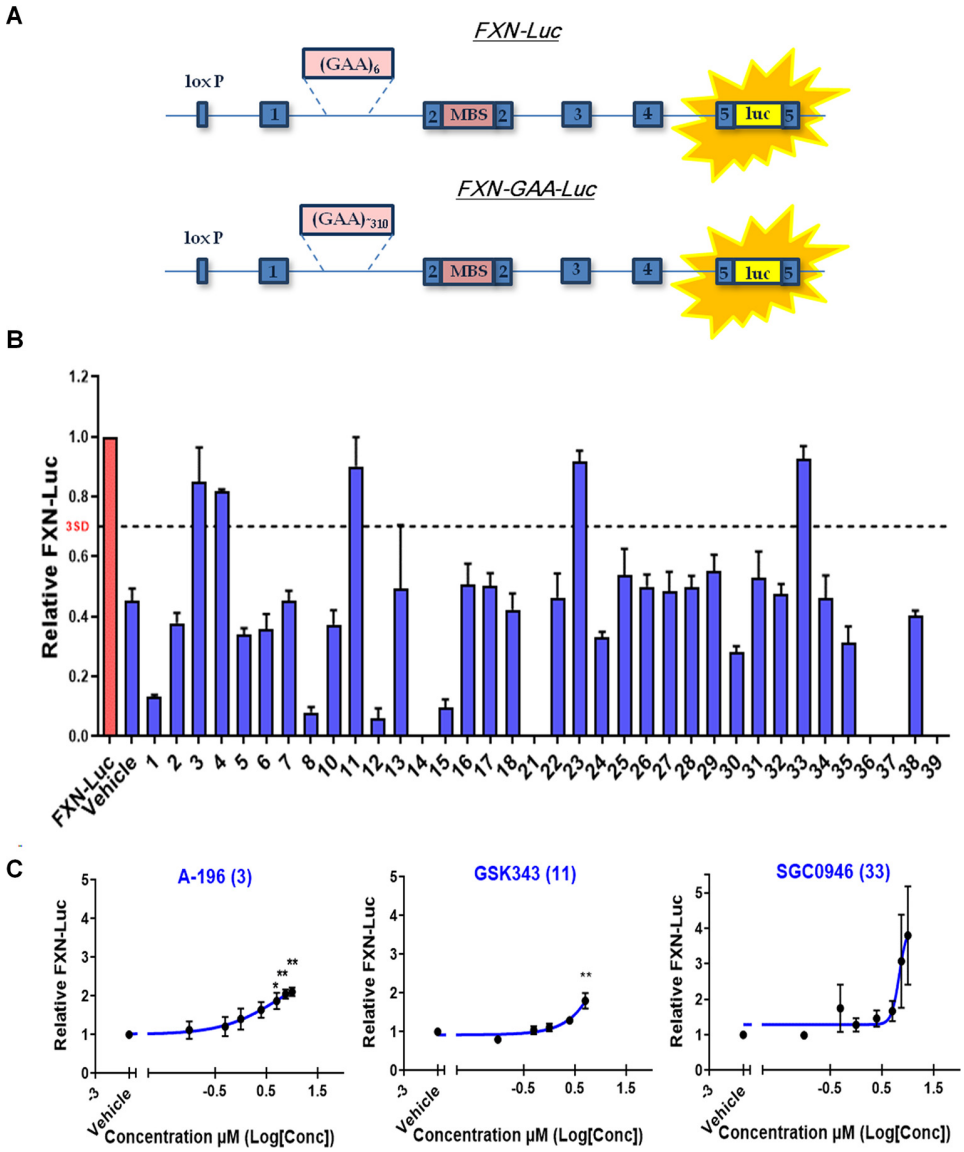

Figure 1. Screening the SGC epigenetic probe set identifies histone methyltransferases as regulators of *FXN* repression. *A*, schematic representation of the *FXN–Luc* and *FXN*–GAA–Luc reporter cell lines. *B*, luciferase assay of the *FXN*–GAA–Luc cell line treated with the SGC epigenetic probes collection. The *FXN–Luc* cell line was used as a reference for FXN levels. *C*, concentration-response curves assessed by luciferase assay of the *FXN*–GAA–Luc cell line treated for 6 days with A-196 EC_{50} 5.2 μM (*left panel*), GSK343 EC_{50} 596 μM (*middle panel*), and SGC0946 EC_{50} 6.8 μM (*right panel*). The data are relative to the vehicle and are presented as means ± S.E.M. ($n = 3$ performed in duplicate, one-way ANOVA followed by Bonferroni test). *, $p < 0.05$; **, $p < 0.01$. *Conc*, concentration, *MBS*, MS2 protein-binding sites, *luc*, luciferase.

increase FXN mRNA expression in the control lines, indicating that the specific inhibition of the SUV4-20 methyltransferases increases frataxin levels only in FRDA patient–derived cells.

Pharmacological inhibition of SUV4-20 decreased H4K20me2/3 and increased H4K20me1 in FRDA patient–derived cells

The mechanism of action of the highly selective histone methyltransferase inhibitor A-196 has been previously described (32), showing that A-196 decreases global levels of the repressive H4K20me2/3 mark while increasing H4K20me1. To better understand how the inhibition of SUV4-20 mediates the up-regulation of *FXN*, we first analyzed the global methylation status of H4K20 in the *FXN*–GAA–Luc cell line after A-196 treatment. In addition to the structural inactive analog SGC2043, we also tested another inactive analog, A-197. As expected, treatment with 5 or 10 μM of A-196, but not with SGC2043 or A-197, decreases H4K20me2/3 with a concomitant increase in H4K20me1 (Fig. 4, *A–D*).

We also tested the effect of A-196 on the H4K20me2/3 and H4K20me1 marks in FRDA patient–derived primary fibroblasts and lymphoblastoid cell lines compared with the inactive control SGC2043. A 6-day treatment with 5 or 10 μM A-196, but not SGC2043, reduced the global levels of H4K20me2/3 and increased the levels of H4K20me1 (Fig. 4, *E* and *F*).

These results provide evidence that the inhibition of SUV4-20 by A-196 reduces global levels of the repressive H4K20me2/3 mark, increases the levels of H4K20me1, and increases *FXN* expression. When levels of H4K20me2/3 are unchanged, as in the case of the treatment with inactive probes, neither H4K20me2/me3, H4K20me1, nor frataxin levels change (Figs.

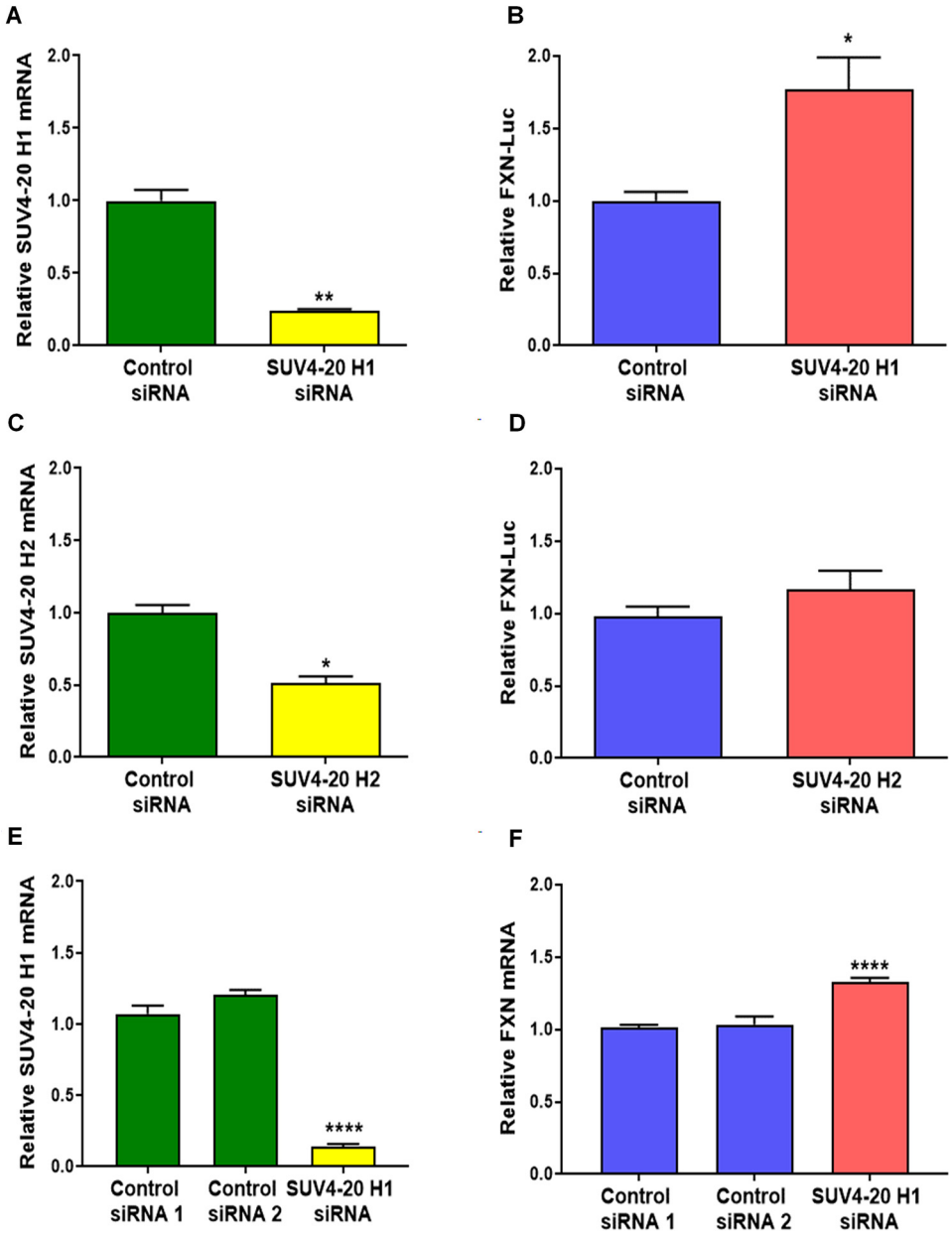

Figure 2. siRNA knockdown of the SUV4-20 family of methyltransferases identifies SUV4-20 H1 as a critical protein for the repression of *FXN*. *A*, relative *SUV4-20 H1* mRNA expression after *SUV4-20 H1* siRNA-mediated knockdown assessed by qRT-PCR. *B*, FXN-Luc protein expression after *SUV4-20 H1* siRNA-mediated knockdown assessed by luciferase assay. *C*, relative *SUV4-20 H2* mRNA expression after *SUV4-20 H2* siRNA-mediated knockdown assessed by qRT-PCR. *D*, FXN-Luc protein expression after *SUV4-20* H2 siRNA-mediated knockdown assessed by luciferase assay. *E*, relative *SUV4-20 H1* mRNA expression after *SUV4-20 H1* knockdown assessed in the fibroblast line GM04078. *F*, relative *FXN* mRNA expression after *SUV4-20H1* down-regulation in fibroblasts GM04078. Experiments performed in the line GM04078 were carried out using two different control siRNA. The data are relative to control siRNA, and control siRNA 1, correspond to 6 days treatments, and are presented as means ± S.E.M. ($n = 3$ performed in triplicate, one-way ANOVA followed by Bonferroni test). *, $p < 0.05$; **, $p < 0.01$; ****, $p < 0.0001$.

3 and 4). These results highlight the importance of H4K20 methylation in the regulation of expression of *FXN* and identify H4K20 methylation as an important histone post-translational modification for FRDA.

Transcriptional perturbation after treatment with A-196 was concentration-dependent and limited to between 1 and 8% of protein-coding genes

Although the inhibition of SUV4-20 results in an increase in *FXN* expression that has potential therapeutic implications for FRDA, this inhibition may alter the epigenome at other loci, resulting in aberrant gene expression elsewhere. Therefore, we treated primary fibroblasts with 1, 5, and 10 μM A-196 for 6 days and analyzed genome-wide perturbations in gene expression caused by the inhibition of SUV4-20 by RNA-Seq. We first assessed *FXN* mRNA expression, confirming an increase in expression (Fig. 5*A*). We then performed principal component analysis (PCA) on the RNA-Seq data and determined that samples treated with A-196 show a concentration-dependent separation along PC1 from untreated, vehicle, and inactive analog-treated samples (Fig. 5*B*). Next, we filtered genes with low read

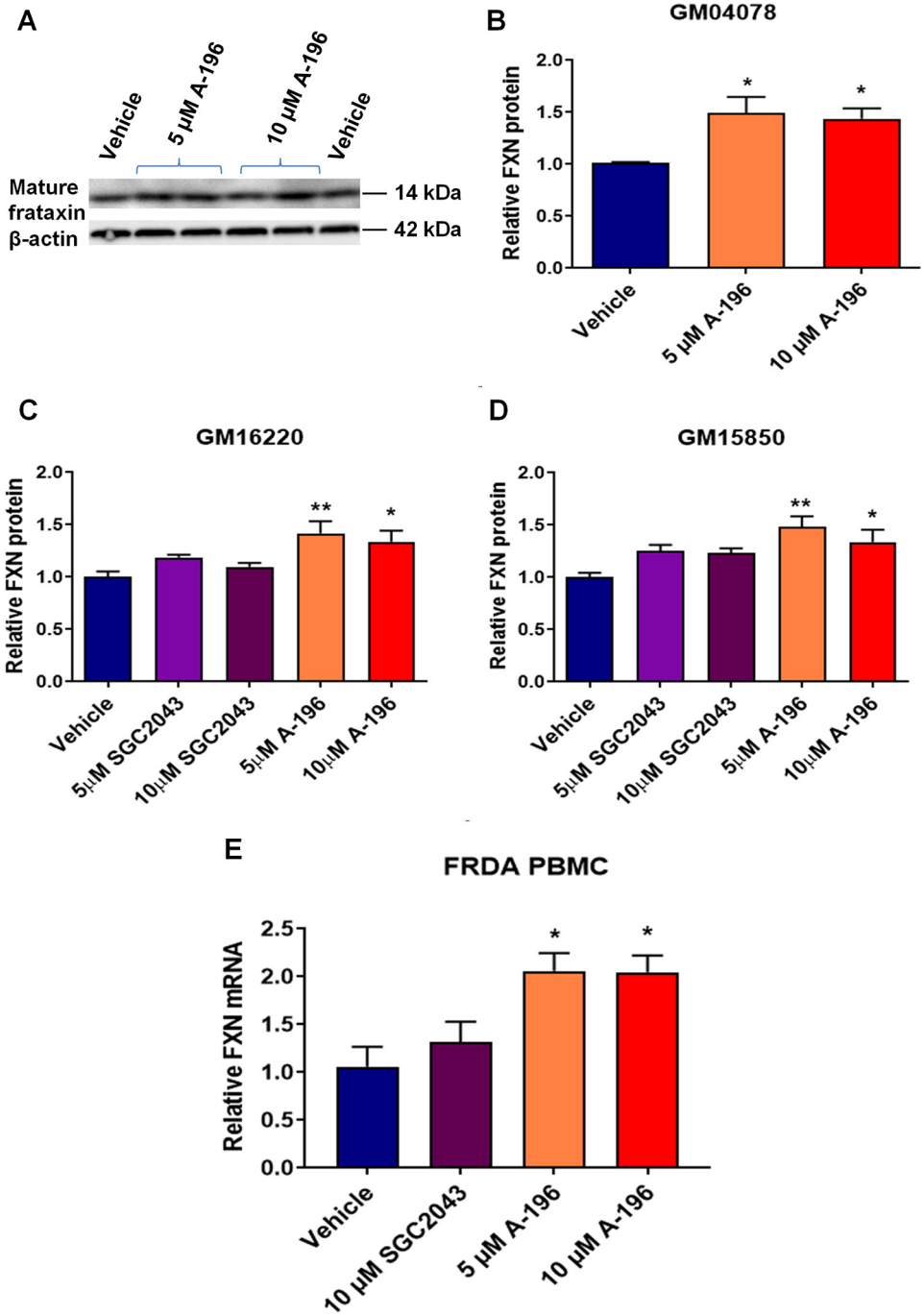

Figure 3. A-196 increases frataxin expression in patient-derived cells. *A*, representative Western blotting of mature frataxin protein expression in the primary fibroblast line GM04078 after A-196 treatment ($n = 3$ in duplicate). *B*, quantification of the experiment shown in *A*. *C* and *D*, relative frataxin protein expression in the lymphoblastoid cell lines GM16220 and GM15850 assessed by AlphaLISA ($n = 4$ in triplicate). *E*, frataxin mRNA expression after A-196 treatment in PBMCs extracted from four FRDA patients. The data are relative to the vehicle, a treatment of 6 days, and are presented as means ± S.E.M. (one-way ANOVA followed by Bonferroni test). *, $p < 0.05$; **, $p < 0.01$.

counts and performed differential gene expression analysis to quantify the extent of transcriptional perturbation. The lowest concentration of A-196 is responsible for 193 DEGs (of ~14,000 genes measured), 5 μM A-196 for 626 DEGs, and 10 μM A-196 for 1098 DEGs (Fig. 5*C*).

We compared our transcriptomics results with previously published data reported from a histone deacetylase inhibitor (HDACi) (33) to measure genome-wide changes in expression. Genome-wide perturbations of expression between compound-treated and control samples were markedly lower in A-196–treated samples (A-196 1–10 μM: 193–1098 DEGs *versus* HDACi 5 μM: 3478 DEGs) (Fig. 5*C*). In addition, the absolute magnitude of expression change by A-196 is lower compared with HDACi (A-196 1–10 μM: 45–67% *versus* HDACi 5 μM: 94%).

No pathways or gene sets were found to be significantly over-represented within genes up-regulated by A-196. In down-

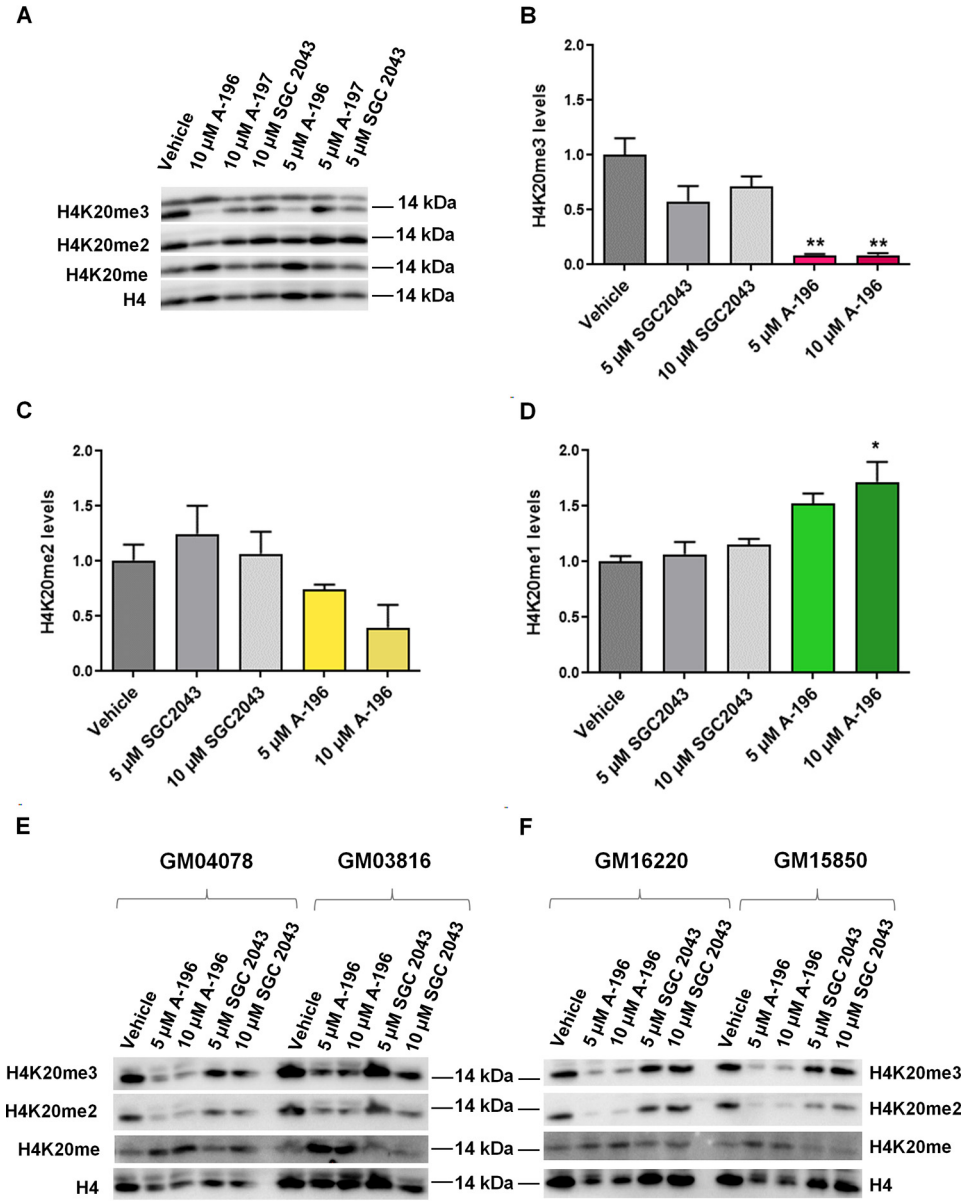

Figure 4. Pharmacological inhibition of the SUV4-20 methyltransferases with A-196 decreases H4K20me2/3 in the *FXN*–GAA–Luc cell line and in FRDA patient–derived cells. *A*, representative Western blotting of the *FXN*–GAA–Luc cell line after A-196, A-197, and SGC2043 treatment. *B–D*, quantification of the global level of H4K20 methylation after inhibition of SUV4-20. *E* and *F*, representative Western blots of patient-derived cells after treatment with the above-mentioned probes. The data are relative to the vehicle, a treatment of 6 days, and are presented as means ± S.E.M. ($n = 3$, one-way ANOVA followed by Bonferroni test). *, $p < 0.05$; **, $p < 0.01$.

regulated genes, collagen fibril organization (GO:0030199) and the endoplasmic reticulum stress response (GO:0034976) are enriched, suggesting some perturbation of these pathways at high concentrations.

Targeting SUV4-20 may promote a transition to an H4K20 monomethylated state, as observed by Schotta *et al.* (34). We examined the expression of 17 key genes that represent affected pathways in this monomethylated state (Table S2). Only two of these genes were differentially expressed using 10 μM A-196 (*CDK1* and *CCNB1*), with no significant perturbation at 5 and 1 μM. Combined with our genome-wide results, this suggests that A-196 is able to promote *FXN* expression with limited unwanted epigenetic effects.

A-196 structural analogs increase FXN expression with improved potency

We sought to improve the potency of A-196 for increasing *FXN* expression through chemical structural modification (supporting information). Information about the structure–activity relationship of A-196 was already known, with certain key structural features identified as being critical for inhibitory activity (32). Examination of the crystal structure of A-196 bound to SUV4-20 H1 (Fig. S7) revealed potential avenues of exploration for synthetic modification. The cyclopentyl moiety occupies a hydrophobic pocket that could be further extended into, whereas the pyridyl group sits in a solvent-exposed region and potentially engages in a hydrogen-bonding interaction, which

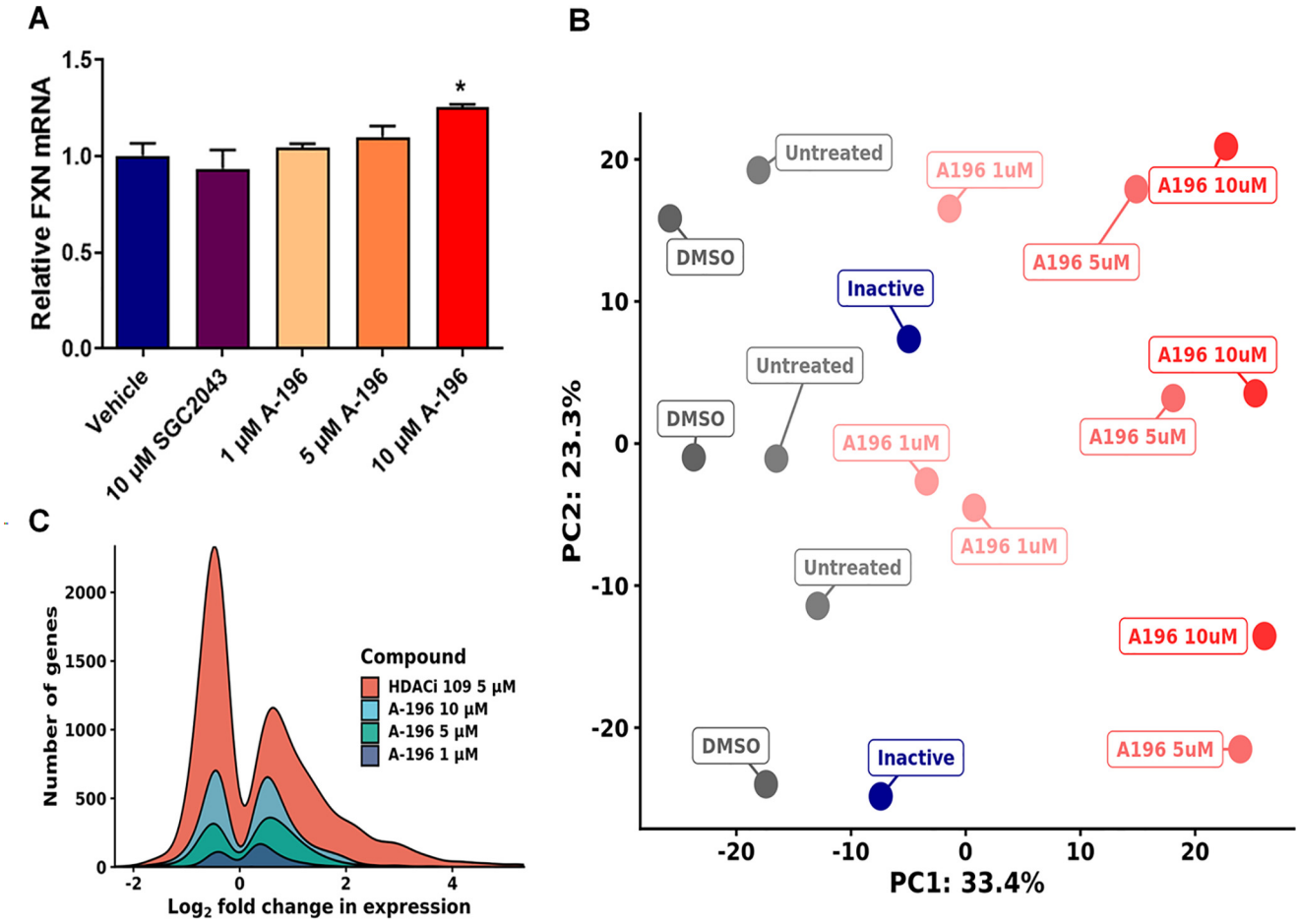

Figure 5. RNA sequencing of primary FRDA fibroblast line GM04078 after A-196 treatment. *A*, relative abundance of *FXN* mRNA in A-196 and SGC2043-treated samples, demonstrating an increase in *FXN* expression. *B*, PCA bi-plot of sequenced samples, illustrating a dose-dependent separation of untreated and A-196–treated samples along PC1. *C*, kernel density plot of significantly differentially expressed genes in all A-196–treated samples and HDACi 109–treated samples from Lai *et al.* (33). A-196 induces significantly lower transcriptional perturbation at all concentrations. The data are relative to the vehicle, a treatment of 6 days and are presented as means ± S.E.M. ($n = 3$, one-way ANOVA followed by Bonferroni test). *, $p < 0.05$.

could be exploited. With this in mind, our efforts primarily focused on increasing lipophilic bulk at the cyclopentyl position, through either further extension into the pocket or increasing ring size. Alongside these modifications, a slight variation of the pyridyl group was also explored, however not as exhaustively as with the upper portion of A-196.

We treated the *FXN*–GAA–Luc cell line for 6 days with 5 μM of each new compound and found that four new molecules (compounds A3, A12, A14, and A15) increased FXN–Luc protein expression to levels comparable with that of A-196 (Fig. 6*A*). These four compounds were also the most potent analogs synthesized, displaying the lowest IC_{50} values against SUV4-20 H1 (Table S3 and Fig. S8). Compounds A3 and A12 exert the strongest effect on FXN–Luc protein expression and also show the greatest difference in potency between SUV4-20 H1 and SUV4-20 H2. Alongside the results of the siRNA-mediated knockdown of SUV4-20 H1 and H2 (Fig. 2, *A–D*), this further suggests an enhanced role for SUV4-20 H1 in FXN expression and may indicate an antagonistic role for SUV4-20 H2 inhibition.

We next performed concentration-response assays using compounds A3 and A12 and confirmed a concentration-dependent increase in FXN–Luc expression after treatment with compounds A3 and A12 (Fig. 6, *B* and *C*). The estimated EC_{50} is 0.21 μM for compound A3 and 2.7 μM for compound A12, compared with 5.2 μM for the starting compound A-196. Finally, we treated patient-derived fibroblasts with compounds A3 and A12 for 6 days and found that compound A3 increased significantly the expression of frataxin mRNA (Fig. 6, *D* and *E*). These structure–activity relationship findings provide proof of concept that other active structural analogs of A-196 also increase *FXN* expression across cell lines and open a new avenue for the potential discovery of clinical lead compounds.

Discussion

Our work builds on the intense research of recent years identifying the epigenetic mechanisms of *FXN* gene silencing in FRDA caused by the GAA repeat expansion in intron 1. Epigenetic silencing of the *FXN* gene is driven by several post-translational modifications of histones (13, 19, 24–31). Here we highlight the role of histone methylation in the regulation of *FXN* expression compared with the more widely studied histone acetylation. We have identified and validated the histone methyltransferase SUV4-20 H1 as a novel therapeutic target for FRDA, first through pharmacological inhibition, and then

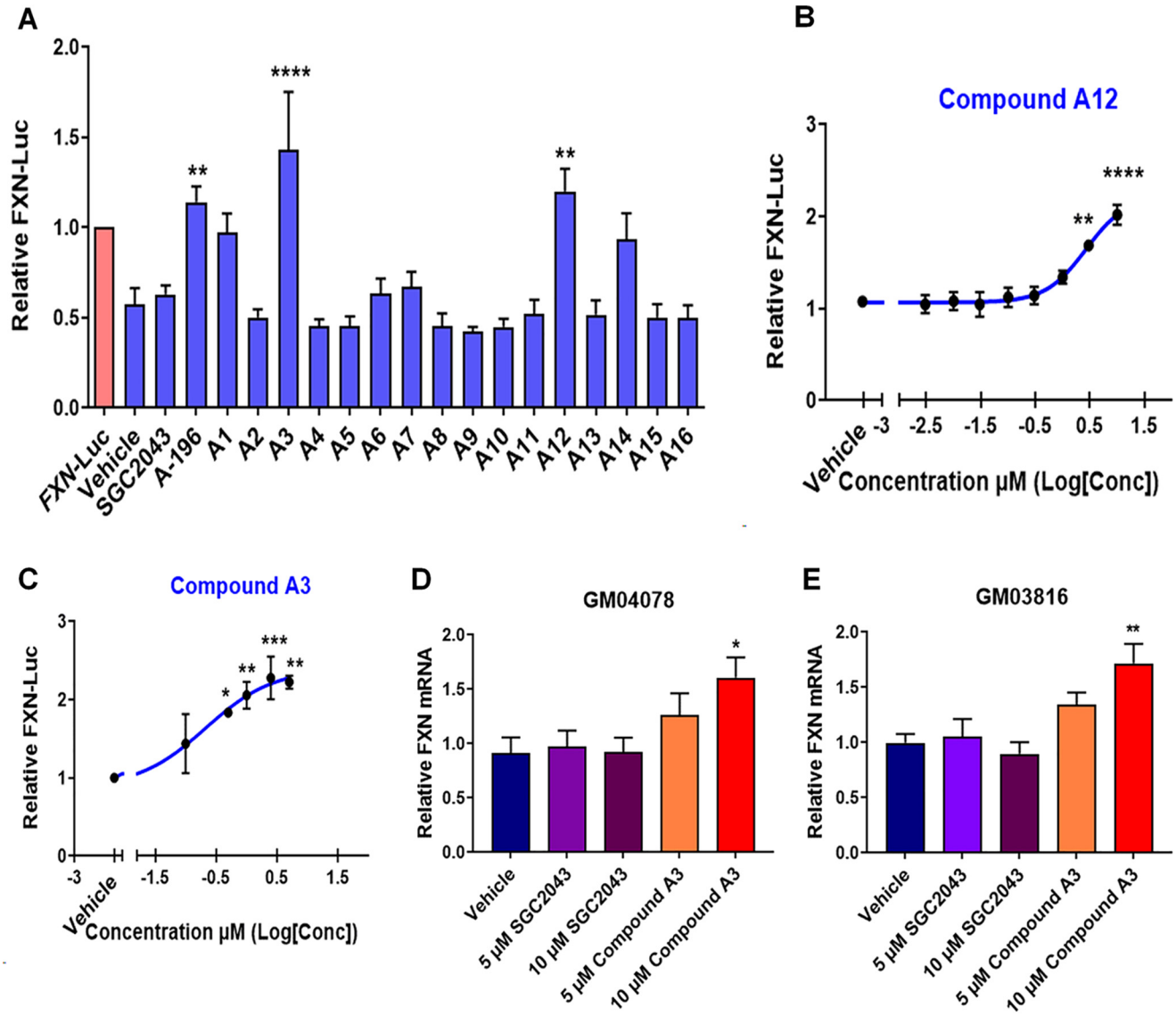

Figure 6. Medicinal chemistry synthesis of new A-196 derivatives capable of increasing frataxin protein expression. *A*, screen of A-196 derivatives using the *FXN*–GAA–Luc cell line ($n = 3$ in triplicate). *B*, concentration-response curve of compound A12 ($EC_{50} = 2.7$ μM) in the line *FXN*–GAA–Luc ($n = 3$ in triplicate). *C*, concentration-response curve of compound A3 ($EC_{50} = 0.21$ μM) in the line *FXN*–GAA–Luc ($n = 3$ in triplicate). *D* and *E*, *FXN* mRNA expression of primary fibroblast GM04078 and GM03816 after treatment with compound A3 ($n = 3$ in duplicate). The data are relative to the vehicle, a treatment of 6 days and are presented as means ± S.E.M. (one-way ANOVA followed by Bonferroni test). *, $p < 0.05$; **, $p < 0.01$; ***, $p < 0.001$; ****, $p < 0.0001$.

siRNA-mediated gene knockdown, in a range of FRDA patient–derived primary cells.

Well-characterized libraries of probe compounds, such as the SGC epigenetic probe set screened here, allow researchers to link selective inhibition of a specific target with a biological response. Screening the SGC epigenetic modifiers allowed us to identify both new mechanisms of epigenetic gene regulation at the *FXN* locus and potential therapeutic targets for the treatment of FRDA. Interestingly, the screen of several inhibitors of chromatin regulatory proteins or domains (bromodomains, demethylases, and methyltransferases) highlighted the role of histone methylation in *FXN* repression. This suggests that modulating the activity of some methyltransferases increases the expression of the partially silenced frataxin gene in FRDA. The majority of the epigenetic modifiers identified by the primary screen were targeted by only one probe compound. However, the library contains three probes for the methyltransferases G9a/GLP (compounds 4, 36, and 37). We identified compound 4 as increasing the expression of FXN–Luc protein, whereas compounds 36 and 37 were toxic at the concentration tested (4 μM), and increased FXN–Luc expression was not observed because of cell death.

The top hit, A-196, is a selective inhibitor of the SUV4-20 methyltransferases (SUV4-20H1 and SUV4-20H2). It has been described to bind selectively to the SUV4-20 enzymes over 29 other methyltransferases, including protein arginine methyltransferases and DNA methyltransferases, a panel of chromatin binders and epigenetic readers, and 125 nonepigenetic targets, which include kinases, G protein–coupled receptors, transporters, and ion channels (32). Previous biochemical and co-crystallization analyses have shown that A-196 is a substrate-competitive inhibitor of both SUV4-20 H1 and H2 enzymes. In cells,

this chemical probe induces a global decrease in di- and trimethylation of H4K20, with a concomitant increase in monomethylation (32). Our results show that this methyltransferase inhibitor produces a significant increase in *FXN* expression in FRDA patient–derived cells. In fibroblasts and lymphocytes, the up-regulation is by ~1.5-fold and in FRDA PBMCs by approximately 2-fold. Asymptomatic carriers of the GAA expansion have only ~50% of the normal levels of frataxin (35), suggesting that even a modest increase in expression may be beneficial for FRDA patients.

The *FXN* gene carrying the disease-associated GAA repeat expansion exhibits increased H4K20me3 in the flanking regions of the GAA repeats (19) and decreased H4K20me1 downstream of the repeats (31). These two methylation marks are regulated by the chemical probe A-196, which has been shown to reduce global levels of H4K20me3 and H4K20me2 while at the same time increasing H4K20me1 (32). Although the siRNA-mediated knockdown of the targets we identify provides evidence of the importance of H4K20 methylation in the regulation of expression of *FXN*, histone lysine methylation and histone arginine methylation have not been extensively studied in FRDA, despite the fact that several reports describe histone methylation marks in the GAA expanded region (17).

To investigate whether A-196 increases FXN expression from the context of the unexpanded chromosomal locus in WT cells, we measured changes in FXN expression after treatment with either 5 or 10 μM A-196 in PBMCs from three control individuals, two control-derived primary fibroblast lines and one control lymphoblastoid cell line and found no increase in expression. It is clear that inhibition of SUV4-20 by A-196 increases FXN expression only in FRDA patient cells carrying GAA expansions and has no effect on WT cells. This is in contrast to the finding that A-196 increased FXN expression from both expanded and nonexpanded *FXN* alleles in the reporter cell line, which may indicate that the *FXN*–Luc model, although carrying a complete 135-kb human *FXN* locus as a bacterial artificial chromosome construct does not perfectly recapitulate the context of the WT endogenous locus.

One of the main concerns of epigenetic therapies is the potential broad biological effects that can result from the global inhibition of an epigenetic target. These effects may be caused by multiple genes that can be transcriptionally controlled by post-translational modifications in histone and nonhistone proteins (36). A-196 demonstrated transcriptional activity that was dose-dependent and substantially reduced compared with a previously reported HDACi (33). There was no evidence of specific pathway activation, suggesting that the transcriptional effects of A-196 do not result in significant changes in cellular function. This activity is most likely due to SUV4-20 inhibition: at 1 and 10 μM, A-196 has been shown to selectively inhibit SUV4-20 (27). No other protein lysine methyltransferases, including the other methyltransferase modifying H4K20, namely SET8, or those that use H3K4, H3K9, H3K27, and H3K79 as substrates, were found to be inhibited by A-196 at that concentration. This high level of specificity is of great importance, and selective inhibitors of specific methyltransferases, if found to modify certain pathologies, may have therapeutic potential with possibly fewer side effects than other epigenetic targets such as HDACs.

Previous studies of FRDA have focused on achieving chromatin remodeling by HDACi (24, 26, 30, 33, 37–44). As opposed to acetyltransferases, lysine methyltransferases have high specificity, modifying usually one single lysine on a single histone. These modifications can lead to either activation or repression of transcription (45). Furthermore, at least 50 nonhistone proteins have been reported to be HDAC substrates, including several transcription factors (RUNX3, p53, c-Myc, nuclear factor κ–light chain enhancer of activated B cells), chaperones (HSP90), signaling mediators (Stat3 and Smad7), and DNA repair proteins (Ku70) (36), which may contribute to potentially detrimental genome-wide effects of HDAC inhibition in patients.

In contrast, lysine methyltransferases have been shown to modify only a few nonhistone substrates (46, 47). Among them, p53 is the most common modified protein, because it can be methylated by the methyltransferases Set7/9 (K372), SMYD2 (K370), G9a (K373), GLP (K373), and SET8 (K382) (46, 48). To the best of our knowledge, among the methyltransferases responsible for the methylation of H4K20, only SET8 (H4K20me1) is able to methylate nonhistone proteins such as p53 and proliferating cell nuclear antigen (47). To date, no studies have reported that either of the SUV4-20 methyltransferases is able to methylate nonhistone proteins, suggesting their selectivity for histones. Moreover, it has been shown that this family of enzymes preferentially methylate histone H4K20 on nucleosomes rather than free histones (20), narrowing down in this way, even more, the epigenetic modification of SUV4-20 genome-wide. The aforementioned characteristics of lysine methyltransferases may be the reason why A-196 used at all tested concentrations modifies the expression of fewer genes compared with HDACi (33).

Although A-196 is highly selective, a caveat for the inhibition of SUV4-20 may be the possible genome-wide transition to an H4K20 monomethylated state. Schotta *et al.* (34) reported in mice that a chromatin-wide transition to H4K20me1 impairs genome integrity and programmed DNA rearrangements and that the complete loss of both SUV4-20 enzymes in *SUV4-20h1*$^{-/-}$ *SUV4-20h2*$^{-/-}$ double-null mice resulted in ablation of nearly all H4K20me3 and H4K20me2, a change incompatible with embryonic development. A genome-wide transition to a monomethylated H4K20 state led to increased sensitivity to damaging stress, with a mechanism that depends on inefficient DNA double-strand break repair and consequent chromosomal aberrations. B cells lacking SUV4-20 were shown to be defective in immunoglobulin class-switch recombination, a process required for antibody isotype diversification. Chemical inhibition of SUV4-20 may, however, be modulated to bypass complete inhibition of these methyltransferases, thus avoiding any aberrant transition of H4K20 methylated states. In support of this, we did not see evidence from our transcriptomic data of A-196 inducing these states and find that unwanted epigenetic activity is even further reduced at the lower doses of 5 and 1 μM.

Improving the potency of A-196 will likely be a strategy to avoid extensive modification of the epigenome, because it will

permit the use of lower doses and limit the risks of off-target effects. Chemical structural modification of A-196 produced compound A3, which according to our estimated EC_{50}, is 24 times more potent than A-196 at inducing *FXN* expression (Figs. 1*C* and 6*C*). New compounds that selectively target SUV4-20 H1 may be important for potentially treating FRDA patients and as important tools to further explore the role of this methyltransferase in other disease states. Our data show that structural modification of A-196 can generate new compounds with the ability to increase *FXN* expression. This increase was observed when using the *FXN*–GAA–Luc cell line, as well as primary fibroblasts, an indication that *FXN* increase in expression is not cell-dependent or limited to a particular cell line.

Experimental procedures

Cell lines

Compound screening was performed using the *FXN*–GAA–Luc reporter cell line with the *FXN*–Luc cell line used as a reference for normal frataxin levels. Both cell lines were built in a HEK293 background as previously described (49) and carry a 135-kb human *FXN* locus (comprising the 80-kb locus spanning exons 1–5b of *FXN* and flanking genomic DNA) with an insertion of the luciferase gene in exon 5a and contain either 6 GAA repeats (*FXN*–Luc) or ~310 GAA repeats (*FXN*–GAA–Luc) in intron 1 of the *FXN* gene. GM04078 (from a clinically FRDA-affected individual carrying alleles with 541 and 420 GAA repeats) and GM03816 (from a clinically FRDA-affected individual carrying alleles with 330 and 380 GAA repeats) are FRDA patient–derived fibroblast lines. GM03440 and GM08402 are control-derived primary fibroblast lines. GM158850 (from a clinically FRDA-affected individual carrying alleles with 650 and 1030 GAA repeats) and GM016220 (from a clinically FRDA-affected individual carrying two alleles each with 460 GAA repeats) are FRDA patient–derived lymphoblastoid cell lines. Finally, GM15851 is a control-derived lymphoblastoid line.

Cell culture

The HEK293 reporter cell lines were cultured in Dulbecco's modified Eagle's medium (DMEM)–high glucose supplemented with 10% fetal bovine serum (FBS), 2 mM L-glutamine, 100 units/ml penicillin/streptomycin, and 100 μg/ml hygromycin B (Life Technologies) (complete DMEM). Fibroblasts lines were obtained from the Coriell Institute (USA) and cultured in minimum essential medium supplemented with 15% FBS, 1% minimum essential medium nonessential amino acid solution (100×, Gibco), and 100 units/ml penicillin/streptomycin. Lymphoblastoid cell lines were also obtained from the Coriell Institute (USA) and cultured in RPMI medium with 15% FBS, 2 mM L-glutamine, and 100 units/ml penicillin/streptomycin. PBMCs were isolated according to Smith *et al.* (50) and cultured in RPMI medium supplemented with 10% FBS, 2 mM L-glutamine, and 100 units/ml penicillin/streptomycin.

Luciferase assay

For assessment of frataxin–luciferase protein expression, the cells were washed with PBS and lysed directly on the plate on ice using the cell culture lysis reagent from the luciferase assay system (Promega, catalog no. E1500). Lysates were transferred to microcentrifuge tubes, vortexed for 15 s, and centrifuged at 12,000 × *g* for 15 s. The supernatant was decanted into a microcentrifuge tube, and 25 μl was loaded in a white opaque 96-well microplate (PerkinElmer). Luciferase expression was determined by measuring luminescence with a PHERAstar FSX microplate reader (BMG LABTECH) equipped with injector pumps, where the injection of 100 μl of luciferase assay reagent was loaded to each sample before measurement. The data were normalized to total protein concentration as determined by BCA protein assay (Thermo Fisher).

Screening the structural genomics consortium epigenetic chemical probes library

FXN–GAA–Luc cells were seeded in 96-well plates at a density of 1.5×10^3 in duplicate and allowed to recover overnight before treatment with the SGC epigenetic probes set. The library was obtained directly from the Structural Genomics Consortium. Concentrations and incubation times are as described in Table S1. The luciferase assay for frataxin–luciferase protein expression was performed as described above.

Western blotting assay

The cells were washed with PBS and lysed directly on the plate on ice with RIPA buffer (50 mM Tris, pH 8, 150 mM NaCl, 2 mM EGTA, 0.5% sodium deoxycholate, 1% Igepal 630, 0.1% SDS with protease inhibitors; Complete Mini, EDTA-free; Roche). The lysates were then transferred to a collection tube and sonicated for a few seconds prior centrifugation for 15 min at 300 × *g* and 4 °C. Protein concentration was determined using a BCA protein assay (Thermo Fisher). The samples were then reduced in Laemmli buffer and incubated for 5 min at 95 °C. 30 μg of protein were resolved for 50 min at 200V on 8–15% SDS-PAGE. Following wet transfer on a polyvinylidene difluoride membrane (Bio-Rad), the samples were incubated with the following antibodies: mouse monoclonal anti-frataxin (Abcam, catalog no. ab113691, 1/1000), rabbit monoclonal anti-EZH1 (Cell Signaling, catalog no. 42088 1/1000), rabbit monoclonal anti-EZH2 (Cell Signaling, catalog no. 5246 1/2500), rabbit polyclonal anti-DOT1L (Abcam, catalog no. ab72454, 1/1000), rabbit polyclonal anti-H4K20me1 (Abcam, catalog no. ab9051, 1/500), rabbit polyclonal anti-H4K20me2 (Abcam,, catalog no. ab9052, 1/2000), rabbit polyclonal anti-H4K20me3 (Abcam, catalog no. ab9053, 1/2000), rabbit polyclonal anti-H4 (Abcam, catalog no. ab10158, 1/2000), and horseradish peroxidase–conjugated anti–β-Actin (Abcam, catalog no. ab49900, 1/25000). Protein quantities were analyzed using the software Image Lab (Bio-Rad).

siRNA-mediated down-regulation of targets

FXN–GAA–Luc cells were counted with an automated cell analyzer NucleoCounter® NC-250TM (ChemoMetec) and

seeded in a 12-well poly-L-lysine–coated plate (12,000 cells/well) in complete DMEM (see Cell culture, as above) minus antibiotics. The cells were then allowed to recover overnight. The next day, the cells were rinsed in Opti-MEM (Gibco 31985047) prior to the liposome delivery. Equal volumes of siRNA and RNAiMAX transfection reagent (Gibco 13778075) were mixed and allowed to form complexes for 20 min. The mix was then added to the cells drop-by-drop and incubated for 6 h. Subsequently, the medium was supplemented with FBS, and the next day, the medium was changed to complete DMEM (see above) minus antibiotics. 6 days post-transfection, the cells were collected for Western blotting, luciferase, and qRT-PCR assays. siRNAs were purchased from Dharmacon as SMARTpool/ON-TARGETplus as follow: SUV4-20 H1 (catalog no. 51111), SUV4-20 H2 (catalog no. 84787), EZH1 (catalog no. 2145), EZH2 (catalog no. 2146), DOT1L (catalog no. 84444), and nontargeting (catalog no. D-001810-10).

Adenylate kinase assay

The adenylate kinase assay (ToxiLight bioassay kit LT07-217; Lonza) to assess toxicity was performed following the instructions of the manufacturer. Briefly, 5 μl of the medium where cells were cultured was transferred to a 384 Greiner LUMITRACTM white plate and allowed to reach room temperature. 25 μl of the adenylate kinase detection reagent were then added to each well and incubated for 5 min. Finally, the plate was read in the PHERAstar FSX microplate reader (BMG LABTECH).

qRT-PCR

Total mRNA was extracted using the RNeasy mini kit (Qiagen) and then treated with RNase-free DNase (Qiagen). 1 μg of RNA was used to synthesize cDNA using random primers (Life Technologies) and SuperScript III reverse transcriptase (Life Technologies) in a 20-μl reaction volume. Quantitative PCR was carried out using primers that can be found in the supporting information. The data were normalized to HRPT1 and analyzed by the $2^{-\Delta\Delta}{}_{Ct}$ method (51).

AlphaLISA assay to quantify human frataxin

The AlphaLISA human frataxin detection kit (PerkinElmer, catalog no. AL322HV/C/F) was scaled down to a white opaque 384-well plate format (PerkinElmer) and adapted from the manufacturer's recommendations. Briefly, an hFXN analyte standard dilution was prepared alongside the samples using the AlphaLISA immunoassay buffer, to which the biotinylated anti-hFXN antibody was added for 1 h at room temperature. AlphaLISA anti-hFXN acceptor beads were added for an additional hour at room temperature, after which streptavidin donor beads solution were put on for a further 2 h at room temperature. Finally, the plate was read using a PHERAstar FSX microplate reader (BMG LABTECH) at a wavelength of 615 nm. The data were normalized for protein quantity using the BCA assay.

RNA sequencing

Total RNA from primary fibroblasts was extracted using the RNeasy mini kit (Qiagen), including DNase I treatment to remove genomic DNA contamination. RNA integrity was determined using the Agilent RNA 6000 Pico kit on a Bioanalyzer. 100 ng of each sample (measured using the Quant-iT RiboGreen RNA assay kit) was submitted for library preparation and sequencing at the Oxford Genomics Centre. Twenty-four strand-specific libraries were prepared from GM04078 and the healthy control line GM03440 using the NEBNext Ultra II mRNA kit following manufacturer's instructions. Sequencing was performed on an Illumina HiSeq 4000 across two lanes, generating 25-33 million read pairs per sample. Reads were pseudoaligned to Ensembl GRCh38 (version 98) cDNA reference using Kallisto (version 0.46.0), with 86–89% alignment. Transcript abundance estimates were summarized to gene-level counts using Tximport (version 1.12.3). Differential gene expression analysis was performed using DESeq2 (version 1.24.0), excluding genes with fewer than 10 counts average across all samples. A false discovery rate cutoff of $\leq$0.01 was used to call differential expression. Principal component analysis was performed using prcomp in R (version 3.6.1). Two GM03440 samples and one GM04078 sample were classed as outliers because of isolated clustering from technical replicates on a PCA bi-plot and were therefore excluded from further analysis (Fig. S9).

Pathway enrichment analysis was performed using gprofiler2 (version 0.1.8), querying the GO Biological Process, Kyoto Encyclopedia of Genes and Genomes, and REACTOME databases. Gene sets larger than 350 were excluded for interpretability. All genes considered for differential expression were used as background, and a false discovery rate cutoff of 0.01 was used.

For comparison between our transcriptomic data and the work by Lai *et al.* (33), raw fastq files were obtained from Sequence Read Archive accession no. PRJNA495860 and processed as described above. The number of replicates per condition was kept constant to minimize differences in statistical power.

Data availability

All data are contained in the article except for RNA-Seq data that are available at the Gene Expression Omnibus under accession number GSE145115.

Acknowledgments—We thank Dr. Ana M. Silva and Dr. Michele M. P. Lufino for the development of the *FXN*–GAA–Luc and *FXN*–Luc reporter cell lines and for advice at the start of this study. We also thank the Oxford Genomics Centre at the Wellcome Centre for Human Genetics (funded by Wellcome Trust Grant 203141/Z/16/Z) for the generation and initial processing of the sequencing data. The SGC Epigenetic Probe Library was supplied by the Structural Genomics Consortium under an Open Science Trust Agreement: http://www.thesgc.org/click-trust.

Author contributions—G. V.-E., R. Q., R. W.-M., and P. E. B. conceptualization; G. V.-E., P. K., and R. M. resources; G. V.-E., P. K.,

and F. L. data curation; G. V.-E., P. K., I. d. M. d. B., A. D., and F. L. formal analysis; G. V.-E., G. C., M. V., A. H. N., P. E. B., and R. W.-M. supervision; G. V.-E., P. E. B., and R. W.-M. funding acquisition; G. V.-E., R. Q., and SS validation; G. V.-E., R. Q., R. M., S. S., I. d. M. d. B., A. D., G. C., and F. L. investigation; G. V.-E. visualization; G. V.-E., S. S., G. C., P. E. B., and R. W.-M. methodology; G. V.-E., R. Q., P. K., and R. W.-M. writing-original draft; G. V.-E. project administration; G. V.-E., R. Q., P. K., F. L., M. V., A. H. N., P. E. B., and R. W.-M. writing-review and editing.

Funding and additional information—This work was supported in part by LifeArc Project 10312. G. V.-E. was supported by the Ecuadorian government through Secretaría Nacional de Educación Superior, Ciencia, Tecnología e Innovación Act 063-CIBAE-2015. R. Q. is grateful to the Engineering and Physical Sciences Research Council Centre for Doctoral Training in Synthesis for Biology and Medicine for Studentship EP/L015838/1. R. Q. was generously supported by AstraZeneca, Diamond Light Source, Defence Science and Technology Laboratory, Evotec, GlaxoSmithKline, Janssen, Novartis, Pfizer, Syngenta, Takeda, Union Chimique Belge, and Vertex. P. E. B. was supported by Alzheimer's Research UK Grant ARUK-2018DDI-OX. The Structural Genomics Consortium (Charity 1097737) receives funds from AbbVie, Bayer Pharma AG, Boehringer Ingelheim, the Canada Foundation for Innovation, the Eshelman Institute for Innovation, Genome Canada, Innovative Medicines Initiative (European Union/European Federation of Pharmaceutical Industries and Associations) under ULTRA-DD Grant 115766, Janssen, Merck, MSD, Novartis Pharma AG, the Ontario Ministry of Economic Development and Innovation, Pfizer, the São Paulo Research Foundation–Fundação de Amparo à Pesquisa do Estado de São Paulo, Takeda, and Wellcome Grant 106169/ZZ14/Z.

Conflict of interest—The authors declare that they have no conflicts of interest with the contents of this article.

Abbreviations—The abbreviations used are: FRDA, Friedreich's ataxia; FXN, frataxin; RNA-Seq, RNA sequencing; SGC, Structural Genomics Consortium; PBMC, peripheral blood mononuclear cell; qRT-PCR, quantitative RT-PCR; PCA, principal component analysis; HDACi, histone deacetylase inhibitor; DEG, differentially expressed gene; DMEM, Dulbecco's modified Eagle's medium; FBS, fetal bovine serum; ANOVA, analysis of variance.

References

1. Campuzano, V., Montermini, L., Moltò, M. D., Pianese, L., Cossée, M., Cavalcanti, F., Monros, E., Rodius, F., Duclos, F., Monticelli, A., Zara, F., Cañizares, J., Koutnikova, H., Sanjay, I., Gellera, C., *et al.* (1996) Friedreich's ataxia: autosomal recessive disease caused by an intronic GAA triplet repeat expansion. *Science* **271,** 1423–1427 CrossRef Medline
2. Cossée, M., Schmitt, M., Campuzano, V., Reutenauer, L., Moutou, C., Mandel, J.-L., and Koenig, M. (1997) Evolution of the Friedreich's ataxia trinucleotide repeat expansion: founder effect and premutations. *Proc. Natl. Acad. Sci. U.S.A.* **94,** 7452–7457 CrossRef Medline
3. Chamberlain, S., Shaw, J., Rowland, A., Wallis, J., South, S., Nakamura, Y., Von Gabain, A., Farrall, M., and Williamson, R. (1988) Mapping of mutation causing Friedreich's ataxia to human chromosome 9. *Nature* **334,** 248–250 CrossRef Medline
4. Pastore, A., and Puccio, H. (2013) Frataxin: a protein in search for a function. *J. Neurochem.* **126,** 43–52 CrossRef Medline
5. Pandolfo, M. (2009) Friedreich ataxia: the clinical picture. *J. Neurol.* **256,** 3–8 CrossRef Medline
6. Dürr, A., Cossee, M., Agid, Y., Campuzano, V., Mignard, C., Penet, C., Mandel, J.-L., Brice, A., and Koenig, M. (1996) Clinical and genetic abnormalities in patients with Friedreich's ataxia. *N. Engl. J. Med.* **335,** 1169–1175 CrossRef Medline
7. Bidichandani, S. I., Ashizawa, T., and Patel, P. I. (1998) The GAA triplet-repeat expansion in Friedreich ataxia interferes with transcription and may be associated with an unusual DNA structure. *Am. J. Hum. Genet.* **62,** 111–121 CrossRef Medline
8. Ohshima, K., Montermini, L., Wells, R. D., and Pandolfo, M. (1998) Inhibitory effects of expanded GAA·TTC triplet repeats from intron I of the Friedreich ataxia gene on transcription and replication *in vivo*. *J. Biol. Chem.* **273,** 14588–14595 CrossRef Medline
9. Sakamoto, N., Chastain, P. D., Parniewski, P., Ohshima, K., Pandolfo, M., Griffith, J. D., and Wells, R. D. (1999) Sticky DNA: self-association properties of long GAA·TTC repeats in R·R·Y triplex structures from Friedreich's attaia. *Mol. Cell* **3,** 465–475 CrossRef Medline
10. Sakamoto, N., Ohshima, K., Montermini, L., Pandolfo, M., and Wells, R. D. (2001) Sticky DNA, a self-associated complex formed at long GAA·TTC repeats in intron 1 of the frataxin gene, inhibits transcription. *J. Biol. Chem.* **276,** 27171–27177 CrossRef Medline
11. Grabczyk, E., and Usdin, K. (2000) The GAA*TTC triplet repeat expanded in Friedreich's ataxia impedes transcription elongation by T7 RNA polymerase in a length and supercoil dependent manner. *Nucleic Acids Res.* **28,** 2815–2822 CrossRef Medline
12. Grabczyk, E., Mancuso, M., and Sammarco, M. C. (2007) A persistent RNA·DNA hybrid formed by transcription of the Friedreich ataxia triplet repeat in live bacteria, and by T7 RNAP *in vitro*. *Nucleic Acids Res.* **35,** 5351–5359 CrossRef Medline
13. Saveliev, A., Everett, C., Sharpe, T., Webster, Z., and Festenstein, R. (2003) DNA triplet repeats mediate heterochromatin–protein-1–sensitive variegated gene silencing. *Nature* **422,** 909–913 CrossRef Medline
14. Greene, E., Mahishi, L., Entezam, A., Kumari, D., and Usdin, K. (2007) Repeat-induced epigenetic changes in intron 1 of the frataxin gene and its consequences in Friedreich ataxia. *Nucleic Acids Res.* **35,** 3383–3390 CrossRef Medline
15. Silva, A. M., Brown, J. M., Buckle, V. J., Wade-Martins, R., and Lufino, M. M. P. (2015) Expanded GAA repeats impair FXN gene expression and reposition the FXN locus to the nuclear lamina in single cells. *Hum. Mol. Genet.* **24,** 3457–3471 CrossRef Medline
16. Nageshwaran, S., and Festenstein, R. (2015) Epigenetics and triplet-repeat neurological diseases. *Front. Neurol.* **6,** 262–9 CrossRef Medline
17. Sandi, C., Sandi, M., Virmouni, S. A., Al-Mahdawi, S., and Pook, M. A. (2014) Epigenetic-based therapies for Friedreich ataxia. *Front. Genet.* **5,** 165 CrossRef Medline
18. Jørgensen, S., Schotta, G., and Sørensen, C. S. (2013) Histone H4 lysine 20 methylation: key player in epigenetic regulation of genomic integrity. *Nucleic Acids Res.* **41,** 2797–2806 CrossRef Medline
19. Kim, E., Napierala, M., and Dent, S. Y. R. (2011) Hyperexpansion of GAA repeats affects post-initiation steps of FXN transcription in Friedreich's ataxia. *Nucleic Acids Res.* **39,** 8366–8377 CrossRef Medline
20. Schotta, G., Lachner, M., Sarma, K., Ebert, A., Sengupta, R., Reuter, G., Reinberg, D., and Jenuwein, T. (2004) A silencing pathway to induce H3-K9 and H4-K20 trimethylation at constitutive heterochromatin. *Genes Dev.* **18,** 1251–1262 CrossRef Medline
21. Ackloo, S., Brown, P. J., and Müller, S. (2017) Chemical probes targeting epigenetic proteins: applications beyond oncology. *Epigenetics* **12,** 378–400 CrossRef Medline
22. Scheer, S., Ackloo, S., Medina, T. S., Schapira, M., Li, F., Ward, J. A., Lewis, A. M., Northrop, J. P., Richardson, P. L., Kaniskan, H. Ü., Shen, Y., Liu, J., Smil, D., McLeod, D., Zepeda-Velazquez, C. A., *et al.* (2019) A chemical biology toolbox to study protein methyltransferases and epigenetic signaling. *Nat. Commun.* **10,** 19 CrossRef Medline
23. Lufino, M. M. P., Silva, A. M., Németh, A. H., Alegre-Abarrategui, J., Russell, A. J., and Wade-Martins, R. (2013) A GAA repeat expansion reporter model of friedreich's ataxia recapitulates the genomic context and allows

rapid screening of therapeutic compounds. *Hum. Mol. Genet.* **22,** 5173–5187 CrossRef Medline

24. Herman, D., Jenssen, K., Burnett, R., Soragni, E., Perlman, S. L., and Gottesfeld, J. M. (2006) Histone deacetylase inhibitors reverse gene silencing in Friedreich's ataxia. *Nat. Chem. Biol.* **2,** 551–558 CrossRef Medline
25. Al-Mahdawi, S., Pinto, R. M., Ismail, O., Varshney, D., Lymperi, S., Sandi, C., Trabzuni, D., and Pook, M. (2008) The Friedreich ataxia GAA repeat expansion mutation induces comparable epigenetic changes in human and transgenic mouse brain and heart tissues. *Hum. Mol. Genet.* **17,** 735–746 CrossRef Medline
26. Rai, M., Soragni, E., Jenssen, K., Burnett, R., Herman, D., Coppola, G., Geschwind, D. H., Gottesfeld, J. M., and Pandolfo, M. (2008) HDAC inhibitors correct frataxin deficiency in a Friedreich ataxia mouse model. *PLoS One* **3,** e1958 CrossRef Medline
27. De Biase, I., Chutake, Y. K., Rindler, P. M., and Bidichandani, S. I. (2009) Epigenetic silencing in Friedreich ataxia is associated with depletion of CTCF (CCCTC-binding factor) and antisense transcription. *PLoS One* **4,** e7914 CrossRef Medline
28. Punga, T., and Bühler, M. (2010) Long intronic GAA repeats causing Friedreich ataxia impede transcription elongation. *EMBO Mol. Med.* **2,** 120–129 CrossRef Medline
29. Kumari, D., Biacsi, R. E., and Usdin, K. (2011) Repeat expansion affects both transcription initiation and elongation in Friedreich ataxia cells. *J. Biol. Chem.* **286,** 4209–4215 CrossRef Medline
30. Chan, P. K., Torres, R., Yandim, C., Law, P. P., Khadayate, S., Mauri, M., Grosan, C., Chapman-Rothe, N., Giunti, P., Pook, M., and Festenstein, R. (2013) Heterochromatinization induced by GAA-repeat hyperexpansion in Friedreich's ataxia can be reduced upon HDAC inhibition by vitamin B_3. *Hum. Mol. Genet.* **22,** 2662–2675 CrossRef Medline
31. Li, Y., Lu, Y., Polak, U., Lin, K., Shen, J., Farmer, J., Seyer, L., Bhalla, A. D., Rozwadowska, N., Lynch, D. R., Butler, J. S., and Napierala, M. (2015) Expanded GAA repeats impede transcription elongation through the FXN gene and induce transcriptional silencing that is restricted to the FXN locus. *Hum. Mol. Genet.* **24,** 6932–6943 CrossRef Medline
32. Bromberg, K. D., Mitchell, T. R. H., Upadhyay, A. K., Jakob, C. G., Jhala, M. A., Comess, K. M., Lasko, L. M., Li, C., Tuzon, C. T., Dai, Y., Li, F., Eram, M. S., Nuber, A., Soni, N. B., Manaves, V., *et al.* (2017) The SUV4-20 inhibitor A-196 verifies a role for epigenetics in genomic integrity. *Nat. Chem. Biol.* **13,** 317–324 CrossRef Medline
33. Lai, J.-I., Nachun, D., Petrosyan, L., Throesch, B., Campau, E., Gao, F., Baldwin, K. K., Coppola, G., Gottesfeld, J. M., and Soragni, E. (2019) Transcriptional profiling of isogenic Friedreich ataxia neurons and effect of an HDAC inhibitor on disease signatures. *J. Biol. Chem.* **294,** 1846–1859 CrossRef Medline
34. Schotta, G., Sengupta, R., Kubicek, S., Malin, S., Kauer, M., Callén, E., Celeste, A., Pagani, M., Opravil, S., De La Rosa-Velazquez, I. A., Espejo, A., Bedford, M. T., Nussenzweig, A., Busslinger, M., and Jenuwein, T. (2008) A chromatin-wide transition to H4K20 monomethylation impairs genome integrity and programmed DNA rearrangements in the mouse. *Genes Dev.* **22,** 2048–2061 CrossRef Medline
35. Campuzano, V., Montermini, L., Lutz, Y., Cova, L., Hindelang, C., Jiralerspong, S., Trottier, Y., Kish, S. J., Faucheux, B., Trouillas, P., Authier, F. J., Dürr, A., Mandel, J. L., Vescovi, A., Pandolfo, M., *et al.* (1997) Frataxin is reduced in Friedreich ataxia patients and is associated with mitochondrial membranes. *Hum. Mol. Genet.* **6,** 1771–1780 CrossRef Medline
36. Kim, H.-J., and Bae, S.-C. (2011) Histone deacetylase inhibitors: molecular mechanisms of action and clinical trials as anti-cancer drugs. *Am. J. Transl. Res.* **3,** 166–179 Medline
37. Soragni, E., Herman, D., Dent, S. Y. R., Gottesfeld, J. M., Wells, R. D., and Napierala, M. (2008) Long intronic GAA·TTC repeats induce epigenetic changes and reporter gene silencing in a molecular model of Friedreich ataxia. *Nucleic Acids Res.* **36,** 6056–6065 CrossRef Medline
38. Codazzi, F., Hu, A., Rai, M., Donatello, S., Salerno Scarzella, F., Mangiameli, E., Pelizzoni, I., Grohovaz, F., and Pandolfo, M. (2016) Friedreich ataxia induced pluripotent stem cell-derived neurons show a cellular phenotype that is corrected by a benzamide HDAC inhibitor. *Hum. Mol. Genet.* **25,** 4847–4855 CrossRef Medline
39. Sandi, C., Pinto, R. M., Al-Mahdawi, S., Ezzatizadeh, V., Barnes, G., Jones, S., Rusche, J. R., Gottesfeld, J. M., and Pook, M. A. (2011) Prolonged treatment with pimelic o-aminobenzamide HDAC inhibitors ameliorates the disease phenotype of a Friedreich ataxia mouse model. *Neurobiol. Dis.* **42,** 496–505 CrossRef Medline
40. Rai, M., Soragni, E., Chou, C. J., Barnes, G., Jones, S., Rusche, J. R., Gottesfeld, J. M., and Pandolfo, M. (2010) Two new pimelic diphenylamide HDAC inhibitors induce sustained frataxin upregulation in cells from Friedreich's ataxia patients and in a mouse model. *PLoS One* **5,** e8825 CrossRef Medline
41. Soragni, E., Chou, C. J., Rusche, J. R., and Gottesfeld, J. M. (2015) Mechanism of action of 2-aminobenzamide HDAC inhibitors in reversing gene silencing in Friedreich's ataxia. *Front. Neurol.* **6,** 44 Medline
42. Chutake, Y. K., Lam, C. C., Costello, W. N., Anderson, M. P., and Bidichandani, S. I. (2016) Reversal of epigenetic promoter silencing in Friedreich ataxia by a class I histone deacetylase inhibitor. *Nucleic Acids Res.* **44,** 5095–5104 CrossRef Medline
43. Xu, C., Soragni, E., Chou, C. J., Herman, D., Plasterer, H. L., Rusche, J. R., and Gottesfeld, J. M. (2009) Chemical probes identify a role for histone deacetylase 3 in Friedreich's ataxia gene silencing. *Chem. Biol.* **16,** 980–989 CrossRef Medline
44. Xu, C., Soragni, E., Jacques, V., Rusche, J. R., and Gottesfeld, J. M. (2011) Improved histone deacetylase inhibitors as therapeutics for the neurodegenerative disease Friedreich's ataxia: a new synthetic route. *Pharmaceuticals (Basel)* **4,** 1578–1590 CrossRef Medline
45. Bannister, A. J., and Kouzarides, T. (2005) Reversing histone methylation. *Nature* **436,** 1103–1106 CrossRef Medline
46. Zhang, X., Wen, H., and Shi, X. (2012) Lysine methylation: beyond histones. *Acta Biochim. Biophys. Sin. (Shanghai)* **44,** 14–27 CrossRef Medline
47. Ümit Kaniskan, H., Martini, M. L., and Jin, J. (2018) Inhibitors of protein methyltransferases and demethylases. *Chem. Rev.* **118,** 989–1068 CrossRef Medline
48. Bissinger, E.-M., Heinke, R., Sippl, W., and Jung, M. (2010) Targeting epigenetic modifiers: inhibitors of histone methyltransferases. *Medchemcomm.* **1,** 114–124 CrossRef
49. Spacey, S. D., Szczygielski, B. I., Young, S. P., Hukin, J., Selby, K., and Snutch, T. P. (2004) Malaysian siblings with friedreich ataxia and chorea: a novel deletion in the frataxin gene. *Can. J. Neurol. Sci.* **31,** 383–386 CrossRef Medline
50. Smith, A. M., Depp, C., Ryan, B. J., Johnston, G. I., Alegre-Abarrategui, J., Evetts, S., Rolinski, M., Baig, F., Ruffmann, C., Simon, A. K., Hu, M. T. M., and Wade-Martins, R. (2018) Mitochondrial dysfunction and increased glycolysis in prodromal and early Parkinson's blood cells. *Mov. Disord.* **33,** 1580–1590
51. Schmittgen, T. D., and Livak, K. J. (2008) Analyzing real-time PCR data by the comparative CT method. *Nat. Protoc.* **3,** 1101–1108 CrossRef Medline